JOURNAL OF INTEGRAL EQUATIONS
AND APPLICATIONS
Volume 23, Number 3, Fall 2011

TWO-SCALE FINITE ELEMENT DISCRETIZATIONS FOR INTEGRODIFFERENTIAL EQUATIONS

HUAJIE CHEN, FANG LIU, NILS REICH,
CHRISTOPH WINTER AND AIHUI ZHOU

Communicated by Giovanni Monegato

ABSTRACT. In this paper we propose and analyze a number of two-scale discretization schemes for integrodifferential equations arising in finance. It is shown theoretically and numerically that the number of degrees of freedom of the two-scale discretization is significantly smaller than that of the standard one-scale finite element approach while at the same time preserving the accuracy of the one-scale discretization. The main idea of these algorithms is to use a coarse grid to approximate the low frequencies and then to use a fine grid to correct the relatively high frequencies. As a result, both the computational time and the storage can be reduced considerably. A combination of wavelet and Lagrangian finite element basis functions is applied to further reduce the complexity arising from the non-locality of the integrodifferential operators.

1. Introduction. In *mathematical finance*, consider a basket of $d \geq 1$ risky assets whose log returns X_t at time $t > 0$ are modeled by a Lévy process $X = \{X_t\}_{t \geq 0}$ with state space $\mathbf{R}^d$. By the fundamental theorem of asset pricing [**17**], the arbitrage free price u of a European contingent claim with payoff function $g(\cdot)$ and maturity $T > 0$ is given by the conditional expectation

$$u(t,x) = \mathbf{E}\left(g(X_T) \ : \ X_t = x\right),$$

2010 AMS *Mathematics subject classification.* Primary 45K05, 65N15, 65N30, 65N55.
Keywords and phrases. Finite elements, infinitesimal generator, two-scale discretization, wavelets.
This work was partially supported by the National Natural Science Foundation of China under grants 10701083, 10871198, 10971059 and 11071265, by the National Basic Research Program of China under grant 2005CB321704 and by the Huber Kudlich Foundation of ETH Zurich.
The third author is the corresponding author.
Received by the editors on March 29, 2009, and in revised form on October 17, 2009.

DOI:10.1216/JIE-2011-23-3-351

under an a priori chosen (risk-neutral) Martingale measure equivalent to the historical measure (see, e.g., [**16, 18**] for measure selection criteria). Deterministic methods to compute $u(T,x)$ are based on the solution of the corresponding backward Kolmogorov equation

$$u_t + \mathcal{A}u = 0, \qquad u|_{t=T} = g, \tag{1.1}$$

where $\mathcal{A}$ denotes the infinitesimal generator of X (see, e.g., [**19, 36**]). For general Lévy processes X, $\mathcal{A}$ is in general the sum of an elliptic second order differential operator which accounts for the diffusion part of the process and a non-local integral operator which corresponds to the jump part of the process. The pricing equation (1.1) has been studied by several authors, e.g., [**3, 10, 24, 31**] for $d = 1$, and [**19, 36**] for $d \geq 2$, where the domain of the infinitesimal generator $\mathcal{A}$ was characterized explicitly as an anisotropic Sobolev space and the corresponding variational problem was shown to be well-posed.

In the present paper we will investigate some finite element schemes for the elliptic integrodifferential equation

$$\mathcal{A}u(x) = f(x),$$

in $\Omega \subset \mathbf{R}^d$ with suitable boundary conditions, and the backward Kolmogorov (parabolic) equation

$$u_t(t,x) + \mathcal{A}u(t,x) = f(t,x),$$

in $(0,T) \times \Omega$ with suitable initial and boundary conditions. In order to solve these two problems using finite elements, there are two main challenges that need to be addressed:

- The "curse of dimension": The number of degrees of freedom on a tensor product finite element mesh of width h in dimension d grows like $\mathcal{O}(h^{-d})$ as $h \to 0$.
- The non-locality of the underlying operator $\mathcal{A}$: The finite element stiffness matrix is dense and thus consists of $\mathcal{O}(h^{-2d})$ non-zero entries.

To overcome these two challenges, wavelet based finite element discretizations of (1.1) were introduced in [**19, 35, 40**] based on a sparse tensor product approach in combination with wavelet compression techniques. The sparse grid method is a powerful tool in the numerical solution of classical partial differential equations (cf., [**4, 5, 22, 46** and references cited therein]) as well as high-dimensional equations arising in

Finance (cf., [**19, 40**]). Under certain conditions on the wavelets' number of vanishing moments, this approach yields asymptotically optimal, essentially dimension-independent complexity $\mathcal{O}(h^{-1}|\log h|^{2(d-1)})$ (see, e.g., [**35**]). For the analysis of general wavelet based finite element methods we refer to [**15, 39, 40**] and the references therein. Construction techniques for arbitrary order spline wavelets on the interval with prescribed number of vanishing moments can be found in [**14, 33**].

Even though a wavelet discretization of (1.1) is proved to be asymptotically optimal of complexity $\mathcal{O}(h^{-1}|\log h|^{2(d-1)})$ for a very general class of non-local operators, the constants involved in the complexity estimates can be significant. More precisely, on rather low but practically important levels of refinement ($h = 2^{-j}$ with $j \leq 8$, say), there often occurs a computational overhead that, especially for local operators, can be reduced considerably by using classical (Lagrangian) finite element basis functions. Following this observation, in this paper we shall split the non-local operator $\mathcal{A}$ and its corresponding bilinear form into a local and a non-local part. Then, to reduce the computational complexity for solving the stationary part of the Kolmogorov equation (1.1), we shall introduce several two-scale approaches, including a basic two-scale discretization scheme and a so-called combination based two-scale discretization scheme (which is explained in more detail in the following paragraph). The algorithms are motivated by the observation that, for a solution to some elliptic problems, low frequency components can be approximated well by a relatively coarse grid, and high frequency components can be computed on a fine grid using local and parallel procedures. Note that the same observation is also crucial in the theory of multigrid and wavelet methods (see, e.g., [**9, 23, 45**]). As we will prove below, from a financial mathematics point of view, low frequency components correspond to the (non-local) jump part of the underlying stochastic process, whereas high frequencies are arising from its (local) diffusion part. The two-scale approach has been used for solving a variety of partial differential equations and integral equations with different types of discretization methods (see, e.g., [**21, 27–30, 32, 42–44**]). The main philosophy behind this paper is that one should treat phenomena of different scales by different tools. In multigrid methods, this kind of idea is used to devise iterative methods for solving a given discretization scheme (see, e.g., [**2, 23, 41**]); while in our approach, we employ this type of idea for designing discretization schemes.

Let us give a little more detailed illustration of the combination based two-scale method on tensor product domains. The main idea of the two-scale finite element combination method is to use a coarse grid to approximate low frequencies and to combine univariate fine and coarse grids to handle high frequencies by parallel procedures. For instance, the complexity of the standard finite element solution $u_{h,h,h}$ is $O(h^{-3})$ in three-dimensional cases. With the same approximation accuracy, the degrees of freedom for getting the two-scale finite element combination approximation $u^h_{H,H,H}$ is only of complexity $O(h^{-2})$ when $H = O(h^{1/2})$ is chosen for the corresponding univariate fine and coarse grids. This approach turns out to be advantageous in two respects. First, the possibility of using existing codes allows the straightforward application of two-scale combination discretization to large scale problems. Second, since the different subproblems can be solved fully in parallel, there is a very elegant and efficient inherent coarse-grain parallelism that makes the two-scale combination discretization perfectly suitable for modern high-performance computers.

The remainder of this paper is organized as follows. In Section 2, we describe the elliptic framework and the space discretizations by means of finite elements and wavelets. In Section 3, we present some two-scale discretization approaches for both elliptic and parabolic problems. In particular, we explain how to combine the wavelets based grid with the two-scale discretization. In Section 4, some numerical results are presented to show the efficiency of the two-scale algorithms. Finally, an appendix is provided.

2. Preliminaries. In mathematical finance, the underlying domain is most often given by $\Omega = \mathbf{R}^d$ ($d \in \mathbf{N}$) representing the log-price space of the assets under consideration. For computation, however, Ω is chosen to be a bounded polygon domain, which is reasonable since the financial problem on $\mathbf{R}^d$ can be localized to the bounded domain very efficiently (cf., [**36**, Section 4.3]). We denote by $L^2(\Omega)$ the usual square integrable functions with inner product $(\cdot,\cdot)$. The standard notation for Sobolev spaces $W^{s,p}(\Omega)$ and their associated norms and seminorms are used (see, e.g., [**8**]). For $p = 2$, we denote $H^s(\Omega) = W^{s,2}(\Omega)$ and the associate norm $\|\cdot\|_{s,\Omega} = |\cdot|_{s,2,\Omega}$. Further, we define the space

$$\widetilde{H}^s(\Omega) = \left\{ u|_\Omega \ : \ u \in H^s(\mathbf{R}^d),\ u|_{\mathbf{R}^d \setminus \Omega} = 0 \right\}, \tag{2.1}$$

which is used for the integrodifferential operators. If $s+1/2 \notin \mathbf{N}$, then $\widetilde{H}^s(\Omega)$ coincides with $H_0^s(\Omega)$, the closure of $C_0^\infty(\Omega)$ with respect to the norm in $H^s(\Omega)$. For simplicity of notations, we will denote $\widetilde{H}^s(\Omega)$ by $H^s(\Omega)$ and the corresponding norm by $\|\cdot\|_{s,\Omega}$ afterwards. The space $H^{-1}(\Omega)$, the dual of $H_0^1(\Omega)$, will also be used.

Throughout this paper, we shall use the letter C (with or without subscripts) to denote a generic positive constant which may stand for different values at its different occurrences. For convenience, the symbol $\lesssim$ will be used in this paper. The notation $A \lesssim B$ means that $A \leq CB$ for some constant C that is independent of mesh parameters.

2.1. An integrodifferential equation. Consider the elliptic problem derived from a Lévy copula process [**19, 25, 36**]:

$$\begin{cases} \mathcal{A}u = f & \text{in } \Omega, \\ u = 0 & \text{on } \partial\Omega, \end{cases} \tag{2.2}$$

where $\mathcal{A}$ is a non-local integrodifferential operator. The variational form of this problem reads: Find $u \in H^1(\Omega)$ such that

$$\mathcal{E}(u,v) = (f,v) \quad \text{for all } v \in H_0^1(\Omega), \tag{2.3}$$

where the bilinear form $\mathcal{E}(\cdot,\cdot)$ is given by:

$$\mathcal{E}(u,v) = (\mathcal{A}u, v) = D(u,v) + J(u,v), \quad u, v \in H^1(\Omega) \tag{2.4}$$

with the diffusion part

$$D(u,v) = \frac{1}{2} \sum_{i,j=1}^{d} \mathcal{Q}_{ij} \int_\Omega \frac{\partial u}{\partial x_i}(x) \frac{\partial v}{\partial x_j}(x)\, dx, \tag{2.5}$$

satisfying that $Q = (\mathcal{Q}_{ij})_{1 \leq i,j \leq d}$ is a symmetric, nonnegative definite matrix and the jump part

$$J(u,v) = -\int_\Omega \int_{\mathbf{R}^d} (u(x+z) - u(x))\, v(x)\, dx\, \nu(dz). \tag{2.6}$$

In (2.6), $\nu(dz)$ is a Lévy measure $\nu(dz) = k(z)\, dz$, where the Lévy density $k(z)$ is given by a Lévy copula as in [**36**]. For the marginal Lévy measures ν_i of $\nu(dz)$ in each coordinate direction we assume:

Assumption 2.1. *The Lévy measures ν_i, $i = 1, \dots, d$, are absolutely continuous with densities k_i that satisfy quasi-stable margins: There are constants $0 < Y_i \leq 1$ and $c_i^+, c_i^- \geq 0$, $c_i^+ + c_i^- > 0$, $i = 1, \dots, d$, such that*

$$
\begin{aligned}
k_i(z) &\gtrsim c_i^- \frac{1}{|z|^{1+Y_i}} 1_{\{z<0\}}(z) + c_i^+ \frac{1}{|z|^{1+Y_i}} 1_{\{0\leq z\}}(z) \quad 0 < |z| \leq 1, \\
k_i(z) &\lesssim c_i^- \frac{1}{|z|^{1+Y_i}} 1_{\{z<0\}}(z) + c_i^+ \frac{1}{|z|^{1+Y_i}} 1_{\{0\leq z\}}(z) \quad 0 < |z| \leq 1.
\end{aligned} \tag{2.7}
$$

Remark 2.1. Assumption 2.1 with $Y_i \leq 1$ $(i = 1, \dots, d)$ on the intensity of the margins' singularities at the origin is required to prove optimal convergence of our numerical schemes below. It is satisfied by many Lévy processes used in financial modeling, for example Kou's model [**26**], Normal Inverse Gaussian processes [**1**], Meixner processes [**38**], and tempered stable or CGMY processes [**7**] with $Y \leq 1$.

The well-posedness of (2.3) is ensured by

Theorem 2.1. *The bilinear form $\mathcal{E}(\cdot,\cdot)$ satisfies a Gårding inequality, i.e., there exist constants $\gamma > 0$ and $c \geq 0$ such that*

$$
\mathcal{E}(u,u) \geq \gamma \|u\|_{1,\Omega}^2 - c\|u\|_{0,\Omega}^2 \quad \text{for all } u \in H^1(\Omega), \tag{2.8}
$$

and is continuous, i.e.,

$$
\mathcal{E}(u,v) \lesssim \|u\|_{1,\Omega} \|v\|_{1,\Omega} \quad \text{for all } u, v \in H^1(\Omega). \tag{2.9}
$$

Proof. See [**36**, Theorem 4.6]. □

Remark 2.2. Using the exponential shift in time $u \mapsto e^{-ct}u$ with $c \geq 0$ in (1.1), we can erase the L^2-term in (2.8). So we may assume that $\mathcal{E}(\cdot,\cdot)$ is coercive on $H^1(\Omega) \times H^1(\Omega)$, i.e., the following holds

$$
\mathcal{E}(u,u) \gtrsim \|u\|_{1,\Omega}^2 \quad \text{for all } u \in H^1(\Omega). \tag{2.10}
$$

For our analysis, we also need to recall the following well-known result:

Lemma 2.1. *The following holds*

$$\|u\|_{1,\Omega}^2 \lesssim D(u,u) \quad \text{for all } u \in H_0^1(\Omega), \tag{2.11}$$

where $D(\cdot,\cdot)$ denotes the Laplace-type bilinear form given by (2.5).

Additionally, from (2.7) we obtain the following crucial lemma.

Lemma 2.2. *For any $u, v \in H^1(\Omega)$ the following holds*

$$|J(u,v)| \lesssim \|u\|_{0,\Omega}\|v\|_{1,\Omega}, \quad \text{and} \quad |J(u,v)| \lesssim \|u\|_{1,\Omega}\|v\|_{0,\Omega}. \tag{2.12}$$

Proof. As shown in [**19**, Section 2] and [**36**, Section 2] (based on [**37**]), in Fourier space the jump part $J(\cdot,\cdot)$ given in (2.6) can be represented by its so-called Fourier symbol $\psi_J(\cdot)$ as follows:

$$J(u,v) = -\int_\Omega \psi_J(\xi)\widehat{u}(\xi)\overline{\widehat{v}(\xi)}\,d\xi,$$

where

$$\psi_J(\xi) := \int_\Omega \left(1 - e^{i\langle \xi, z\rangle} + i\langle \xi, z\rangle 1_{\{|z|\le 1\}}\right)\nu(dz),$$

and $\widehat{u}$, $\widehat{v}$ denote the Fourier transforms of u and v.

By [**19**, Theorem 3.4] and [**36**, Proposition 3.5], assumption (2.7) implies that ψ_J is equivalent to an anisotropic distance function that satisfies $\psi_J(\xi) \ge 0$ for all $\xi \in \Omega$ and furthermore

$$\psi_J(\xi) \lesssim |\xi_1|^{Y_1} + \cdots + |\xi_d|^{Y_d} + 1$$

with $Y_1, \ldots, Y_d$ given by (2.7). Denoting $\overline{Y} = \max\{Y_1, \ldots, Y_d\}$, we thus obtain

$$\psi_J(\xi) \lesssim (1 + |\xi|^2)^{\overline{Y}/2} \lesssim (1 + |\xi|^2)^{1/2} \quad \text{for all } \xi \in \mathbf{R}^d,$$

where the last inequality follows from (2.7). Hence, using the Cauchy-Schwarz inequality and Plancherel's theorem, we obtain

$$\begin{aligned} |J(u,v)|^2 &\lesssim \int_\Omega |\widehat{u}(\xi)|^2 d\xi \cdot \int_\Omega |\psi_J(\xi)\overline{\widehat{v}(\xi)}|^2 d\xi \\ &\lesssim \|\widehat{u}\|_{0,\Omega}^2 \cdot \int_\Omega (1+|\xi|^2)|\widehat{v}(\xi)|^2 d\xi \\ &\lesssim \|u\|_{0,\Omega}^2 \cdot \|v\|_{1,\Omega}^2. \end{aligned} \tag{2.13}$$

Note that even though the bilinear form $J(\cdot,\cdot)$ is not necessarily symmetric, one may still interchange $\widehat{u}(\xi)$ and $\overline{\widehat{v}(\xi)}$ in (2.13) to obtain

$$|J(u,v)|^2 \lesssim \|u\|_{1,\Omega}^2 \cdot \|v\|_{0,\Omega}^2.$$

This completes the proof. □

2.2. Finite element approximation. In order to discretize the variational equation (2.3), we employ a sequence of piecewise polynomial finite element spaces associated with a shape-regular finite element mesh. Assume that $T^h(\Omega) = \{\tau\} = \{\tau_i\}_i$ is a mesh of Ω with mesh-size function $h(x)$ whose value is the diameter h_τ of the element τ containing x. One basic assumption on the mesh is that it is not exceedingly over-refined locally, namely,

Assumption 2.2. *There exists a $\sigma \geq 1$ such that*

$$h_\Omega^\sigma \lesssim h(x), \quad x \in \Omega, \tag{2.14}$$

where $h_\Omega = \max_{x\in\Omega} h(x)$ is the (largest) mesh size of $T^h(\Omega)$.

This is obviously a very mild assumption from the theoretical point of view. Usually, we will drop the subscript and simply write h instead of h_Ω for the mesh size on a domain that is clear from the context.

Let $T^h(\Omega)$ consist of shape-regular simplices, and define $S^{h,r}(\Omega)$ to be a space of continuous functions on Ω such that for $v \in S^{h,r}(\Omega)$, the restriction of v to each $\tau \in T^h(\Omega)$ is a polynomial of total degree $\leq r$, namely,

$$S^{h,r}(\Omega) = \{v \in C(\overline{\Omega}) : v\,|_\tau \in P_\tau^r \quad \text{for all } \tau \in T^h(\Omega)\}, \tag{2.15}$$

where P_τ^r is the space of polynomials of degree not greater than a positive integer r. Set $S_0^{h,r}(\Omega) = S^{h,r}(\Omega) \cap H_0^1(\Omega)$. These are the Lagrange finite element spaces, and we refer to [**8, 43**] for their basic properties that will be used in our analysis. For simplicity, in this paper we shall focus our study only on the piecewise linear Lagrange finite element approximation. Let $S^h(\Omega) = S^{h,1}(\Omega)$ and $S_0^h(\Omega) = S_0^{h,1}(\Omega)$.

Note that the analysis of this work does not depend on the particular choice of piecewise linear basis functions for $S_0^h(\Omega)$. For instance, one may choose a classical Lagrangian ("nodal") finite element bases (see, e.g., [**8**, Section II.7]) or piecewise linear wavelet basis functions (see, e.g., [**9**, Chapter 1]). In particular, if Ω is a tensor product domain, choosing a wavelet basis for $S_0^h(\Omega)$ allows for the very efficient discretization of the non-local part $J(\cdot,\cdot)$ of $\mathcal{E}(\cdot,\cdot)$ as described in [**19, 35, 39, 40**].

The (standard) one-scale finite element discretization for (2.3) reads: Find $u_h \in S_0^h(\Omega)$ such that

$$\mathcal{E}(u_h, v) = (f, v) \quad \text{for all } v \in S_0^h(\Omega). \tag{2.16}$$

We also require the Galerkin-projection $P_h : H_0^1(\Omega) \to S_0^h(\Omega)$, defined by

$$\mathcal{E}(u - P_h u, v) = 0 \quad \text{for all } v \in S_0^h(\Omega). \tag{2.17}$$

Using the coercivity (2.10) of $\mathcal{E}(\cdot,\cdot)$ and (2.9), one obtains the following well-known error bounds (see, e.g., [**8**, Chapter III]):

Theorem 2.2. *If $u_h \in S_0^h(\Omega)$ is the solution of* (2.16) *and $u \in H^2(\Omega)$, then*

$$\|u - u_h\|_{1,\Omega} \lesssim h|u|_{2,\Omega}, \tag{2.18}$$

$$\|u - u_h\|_{0,\Omega} \lesssim h^2|u|_{2,\Omega}. \tag{2.19}$$

2.3. Wavelets setting. We briefly illustrate how one may use a wavelet basis to discretize the problem. Assume that any meshwidth under consideration can be represented by a negative power of two, and we therefore can associate a level index $j > 0$ to each meshwidth

$h = 2^{-j}$. Denoting $h_0 = 2^0, h_1 = 2^{-1}, h_2 = 2^{-2}, \ldots$, one obtains that the spaces

$$S_0^{h_0}(\Omega) \subset S_0^{h_1}(\Omega) \subset S_0^{h_2}(\Omega) \subset \cdots \subset L^2(\Omega)$$

define a multiresolution in the sense of [**9, 12**]. The spaces $S_0^{h_j}(\Omega) = \text{span}\,(\Phi_j)$, $j = 0, 1, 2, \ldots$, are spanned by single scale bases $\Phi_j = \{\phi_{j,k} : k \in \Delta_j\}$ consisting of the Lagrangian finite element ("nodal") basis functions $\phi_{j,k}$, where Δ_j denotes a suitable index set of cardinality $\dim\,(S_0^{h_j}(\Omega))$.

Using the methodology of [**14, 33**] to the collections Φ_j, one can associate a set of dual bases $\widetilde{\Phi}_j = \{\widetilde{\phi}_{j,k} : k \in \Delta_j\}$, i.e., one has $(\phi_{j,k}, \widetilde{\phi}_{j,k'}) = \delta_{k,k'}$, $k, k' \in \Delta_j$. With $\nabla_j = \Delta_{j+1} \backslash \Delta_j$, for these single-scale bases one can then construct a biorthogonal complement or wavelet bases $\Psi_j = \{\psi_{j,k} : k \in \nabla_j\}$, $\widetilde{\Psi}_j = \{\widetilde{\psi}_{j,k} : k \in \nabla_j\}$, i.e., $(\psi_{j,k}, \widetilde{\psi}_{j',k'}) = \delta_{(j,k),(j',k')}$.

Denoting by W^j the span of Ψ_j the following holds

$$S_0^{h_{j+1}}(\Omega) = W^j \oplus S_0^{h_j}(\Omega), \quad j > 0. \tag{2.20}$$

Thus, for any $j > 0$, the finite element space $S_0^{h_j}(\Omega)$ can be written as a direct sum of the wavelet spaces $W^{j'}$, $j' < j$, (using the convention $W^0 := S_0^{h_0}(\Omega)$).

By (2.20), for any $u_j \in S_0^{h_j}(\Omega)$ one has two equivalent representations

$$u_j = \sum_{j'=0}^{j-1} \sum_{k' \in \nabla_{j'}} d_{j',k'} \psi_{j',k'} = \sum_{k \in \Delta_j} c_k \phi_{j,k}. \tag{2.21}$$

The corresponding arrays of single-scale, respectively wavelet coefficients $\mathbf{c}, \mathbf{d}$ are interrelated by the explicitly known multiscale transformation $\mathbf{T}_j : \mathbf{d} \mapsto \mathbf{c}$ (cf., e.g., [**12**]). Based on the constructions in [**14, 33**] one readily infers that $\bigcup_{j'<j} \Psi_{j'}$ $(j > 0)$ forms a Riesz-basis in $L^2(\Omega)$, i.e., the following holds

$$\|u_j\|^2 \sim \sum_{j'=0}^{j-1} \sum_{k' \in \nabla_{j'}} d_{j',k'}^2 \quad \text{for all } u_j \in S_0^{h_j}(\Omega).$$

Thus, by [**6, 11**], the following holds

$$\|\mathbf{T}_j\|, \|\mathbf{T}_j^{-1}\| = \mathcal{O}(1),$$

which is crucial for the realizations of the Wavelet-Lagrangian two-scale schemes that we describe in Section 3.

2.4. Example of wavelets. As illustrated in [**9**, Section 2.11] and [**14, 33**], one can construct several different wavelet bases for $S_0^{h_j}(\Omega)$ $(j \geq 0)$, depending on which properties are desired. For example, one may obtain wavelets with an arbitrarily large number of vanishing moments, which is very desirable for the compression of non-local operators (cf., e.g., [**13, 35**]). Increasing the number of vanishing moments however expands the wavelets' supports.

Wavelets of arbitrary order on the interval have been constructed in [**14**] in a very sophisticated way; we refer to this source for further details. Furthermore, to illustrate one possible choice of wavelet basis, in dimension $d = 1$, we give an explicit example of a piecewise linear wavelet basis with two vanishing moments which has turned out to be very useful in practice (multivariate wavelets on $[0,1]^d$ can be obtained as suitable tensor products of these).

The wavelets are comprised of piecewise linear continuous functions on $[0,1]$ vanishing at the endpoints. The mesh for level $j \geq 0$ is defined by the nodes $x_{j,k} := k2^{-(j+1)}$ with $k \in \Delta_j := \{0, \ldots, 2^{j+1}\}$. There holds $N_j := \dim(S_0^{h_j}(\Omega)) = 2^{j+1} - 1$ and therefore $M_j := \dim \Psi_j = \dim(S_0^{h_j}(\Omega)) - \dim(S_0^{h_{j-1}}(\Omega)) = 2^j$.

On level $j = 0$ we have $N_0 = M_0 = 1$ and $\psi_{0,1}$ is defined as the piecewise linear function with value $c_0 := \sqrt{3}/2 > 0$ at $x_{0,1} = 1/2$ and 0 at the endpoints 0, 1. This choice of c_0 ensures the L^2 normalization of the wavelets. For $j > 0$ we firstly define $c_j := c_0 2^{j/2}$. Then the boundary wavelet $\psi_{j,0}$ is defined as the piecewise linear function such that $\psi_{j,0}(x_{j,1}) = 2c_j$, $\psi_{j,0}(x_{j,2}) = -c_j$ and $\psi_{j,0}(x_{j,s}) = 0$ for all other $s \neq 1, 2$. Similarly, the boundary wavelet ψ_{j,M_j-1} takes values $\psi_{j,M_j-1}(x_{j,N_j}) = 2c_j$, $\psi_{j,M_j-1}(x_{j,N_j-1}) = -c_j$ and zero at all other nodes. For the remaining location indices $0 < k < M_j - 1$ the wavelet $\psi_{j,k}$ is defined by $\psi_{j,k}(x_{j,2k}) = -c_j$, $\psi_{j,k}(x_{j,2k+1}) = 2c_j$, $\psi_{j,k}(x_{j,2k+2}) = -c_j$ and $\psi_{j,k}(x_{j,s}) = 0$ for all other $s \neq 2k, 2k+1, 2k+2$.

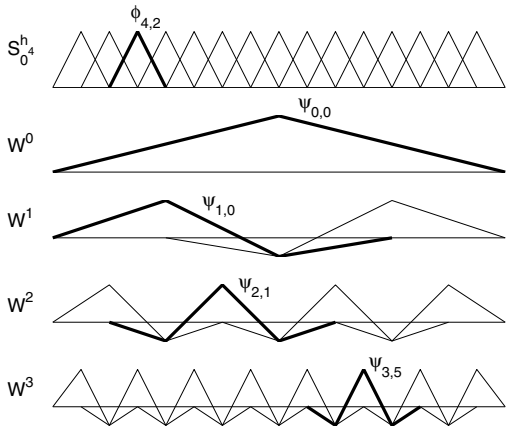

FIGURE 1. Schematic of single-scale space $S_0^{h_j}(\Omega)$ and its decomposition into multiscale wavelet spaces $W^{j'}$.

Since the corresponding dual wavelet bases $\widetilde{\Psi}_j$ $(j \geq 0)$ are solely of analytic importance and do not have to be computed in practice, for the sake of brevity we refer to [**9**] for their illustration.

Figure 1 shows the decomposition of the finite element space $S_0^{h_j}(\Omega)$ $(j = 4)$ spanned by continuous, piecewise linear ("nodal") Lagrangian basis functions $\phi_{j,k}$ into its increment spaces $W^{j'}$, $j' = 0, \ldots, 3$, spanned by the wavelets defined above.

3. Two-scale discretizations. Due to the non-locality of $\mathcal{E}(\cdot,\cdot)$, the straightforward finite element discretization of (2.16) yields a dense matrix of substantial size, which usually is not practicable to implement when Ω has a high dimension. In order to reduce the computational cost of solving the elliptic problem (2.3) and further the parabolic problem, we may introduce some two-scale discretization algorithms.

3.1. A basic two-scale discretization. In this subsection, we may introduce a so-called basic two-scale method. The main idea is to use a coarse mesh of size H, to approximate the low frequencies and to use a fine mesh of size h $(h \ll H)$ to handle the high frequencies

(cf., [**42, 43**]). Based on (2.4), Theorem 2.1, Lemmas 2.1 and 2.2, we may indeed treat $J(\cdot,\cdot)$ as a low frequency perturbation of the high frequency part $D(\cdot,\cdot)$ of $\mathcal{E}(\cdot,\cdot)$. More precisely, for $h \ll H$ our basic two-scale algorithm is defined as follows:

Algorithm 3.1.

1. *Solve* (2.3) *on a coarse grid*: *Find* $u_H \in S_0^H(\Omega)$ *such that*

$$\mathcal{E}(u_H, v) = (f, v) \quad \textit{for all } v \in S_0^H(\Omega).$$

2. *Solve a linear boundary value problem on a fine grid*: *Find* $u^h \in S_0^h(\Omega)$ *such that*

$$D(u^h, v) = (f, v) - J(u_H, v) \quad \textit{for all } v \in S_0^h(\Omega).$$

3. *Find a further coarse grid correction* $e_H \in S_0^H(\Omega)$ *such that*

$$\mathcal{E}(e_H, v) = (f, v) - \mathcal{E}(u^h, v) \quad \textit{for all } v \in S_0^H(\Omega)$$

and set $\widetilde{u}^h = u^h + e_H$ *in* Ω.

Theorem 3.1. *Assume that* u^h *and* $\widetilde{u}^h$ *are obtained by Algorithm* 3.1. *If* $u \in H^2(\Omega)$, *then*

$$\|u^h - u_h\|_{1,\Omega} \lesssim H^2 |u|_{2,\Omega}, \tag{3.1}$$

$$\|\widetilde{u}^h - u_h\|_{0,\Omega} \lesssim H^3 |u|_{2,\Omega}, \tag{3.2}$$

where u_h *denotes the solution of the one-scale discretization* (2.16). *Consequently,*

$$\|u - u^h\|_{1,\Omega} \lesssim (h + H^2)|u|_{2,\Omega}, \tag{3.3}$$

$$\|u - \widetilde{u}^h\|_{0,\Omega} \lesssim (h^2 + H^3)|u|_{2,\Omega}. \tag{3.4}$$

Proof. From (2.16), we have

$$D(u_h, v) + J(u_h, v) = (f, v) \quad \text{for all } v \in S_0^h(\Omega),$$

which together with Lemma 2.2 implies

$$D(u^h - u_h, v) = -J(u_H - u_h, v) \lesssim \|u_H - u_h\|_{0,\Omega}\|v\|_{1,\Omega},$$
$$\text{for all } v \in S_0^h(\Omega).$$

Using Theorem 2.2, we then obtain

$$\begin{aligned}\|u^h - u_h\|_{1,\Omega}^2 &\lesssim D(u^h - u_h, u^h - u_h)\\ &\lesssim \|u_H - u_h\|_{0,\Omega}\|u^h - u_h\|_{1,\Omega}\\ &\lesssim H^2|u|_{2,\Omega}\|u^h - u_h\|_{1,\Omega}.\end{aligned}$$

Hence, we get (3.1). Note that the following holds

$$\begin{aligned}\|\widetilde{u}^h - u_h\|_{0,\Omega} &= \|(I - P_H)(u^h - u_h)\|_{0,\Omega}\\ &\lesssim H\|u^h - u_h\|_{1,\Omega}\\ &\lesssim H^3|u|_{2,\Omega},\end{aligned}$$

where I denotes the identity operator. By Theorem 2.2 and the triangle inequality, we obtain (3.3) and (3.4). This completes the proof. □

Remark 3.1. If, instead of the finite element space $S_0^h(\Omega)$ with piecewise linear basis functions, one chooses a higher order basis, i.e., $S_0^{h,r}(\Omega)$ $(r \geq 1)$ with the mesh of size h, then it can be seen from the above arguments that the solutions u^h and $\widetilde{u}^h$ of the corresponding basic two-scale Algorithm 3.1 satisfy

$$\begin{aligned}\|u - u^h\|_{1,\Omega} &\lesssim (h^r + H^{r+1})|u|_{r+1,\Omega},\\ \|u - \widetilde{u}^h\|_{0,\Omega} &\lesssim (h^{r+1} + H^{r+2})|u|_{r+1,\Omega},\end{aligned}$$

when $u \in H^{r+1}(\Omega)$. Naturally, in this case one may choose Lagrangian finite element basis functions of order r or piecewise polynomial wavelets of degree r to generate $S_0^{h,r}(\Omega)$ (see, e.g., [**14**] for the construction of higher order wavelets on the interval).

Remark 3.2. Based on the two-scale discretizations, we can construct certain local and parallel algorithms to reduce the computational cost even further (see, e.g., [**29**]).

3.2. A combination based two-scale discretization. In this subsection, we shall discuss a combination based two-scale finite element discretization to reduce the computational complexity further over tensor product domains. For the sake of brevity, we only give a detailed description of three-dimensional problems over the domain $\Omega = [0,1]^3$ here. The extension to $\Omega = [0,1]^d$ $(d \geq 2)$ is addressed at the end of this section. The results in this section can easily be generalized to domains like $[-R,R]^d$ $(R > 0)$. Note that such tensor product domains arise in most of the classical asset pricing problems (cf., e.g., [**10, 19**]).

In our discussion, we require a so-called mixed Sobolev space (see, e.g., [**28, 34**]):

$$W_2^{G,3}(\Omega) := \{w \in H^2(\Omega) \ : \ \partial_{x_i}\partial_{x_j}\partial_{x_k}(w) \in L^2(\Omega), i,j,k = 1,\ldots, d,\ x_i \neq x_j \text{ or } x_i \neq x_k\}$$

with its natural norm $\|\cdot\|_{W_2^{G,3}(\Omega)}$. In this notation similar spaces have already been introduced in [**34**].

Furthermore, we shall introduce a two-scale finite element combination approximation for the three-dimensional case. Assume that $T^{h_{x_i}}([0,1])$ is a uniform mesh with mesh size h_{x_i} on $[0,1]$ where $i = 1,2,3$. Set $T^{h_{x_1},h_{x_2},h_{x_3}}(\Omega) = T^{h_{x_1}}([0,1]) \times T^{h_{x_2}}([0,1]) \times T^{h_{x_3}}([0,1])$ is the tensor product mesh. Let $S_0^{h_{x_1},h_{x_2},h_{x_3}}(\Omega) \in H_0^1(\Omega)$ be the standard trilinear finite element space associated with the finite element mesh $T^{h_{x_1},h_{x_2},h_{x_3}}(\Omega)$. Then the standard trilinear finite element scheme on Ω is: Find $u_{h_{x_1},h_{x_2},h_{x_3}} \in S_0^{h_{x_1},h_{x_2},h_{x_3}}(\Omega)$ such that

$$\mathcal{E}(u_{h_{x_1},h_{x_2},h_{x_3}}, v) = (f,v) \quad \text{for all } v \in S_0^{h_{x_1},h_{x_2},h_{x_3}}(\Omega). \tag{3.5}$$

Following [**28, 29**], we may define a two-scale finite element combination approximation $u_{H,H,H}^h$ by

$$u_{H,H,H}^h = u_{h,H,H} + u_{H,h,H} + u_{H,H,h} - 2u_{H,H,H}. \tag{3.6}$$

Theorem 3.2. *If $u \in H_0^1(\Omega) \cap W_2^{G,3}(\Omega)$, then*

$$\|u_{h,h,h} - u_{H,H,H}^h\|_{1,\Omega} \lesssim H^2 \|u\|_{W_2^{G,3}(\Omega)}, \tag{3.7}$$

$$\|u_{h,h,h} - u_{H,H,H}^h\|_{0,\Omega} \lesssim H^3 \|u\|_{W_2^{G,3}(\Omega)}. \tag{3.8}$$

Consequently,

$$\|u - u^h_{H,H,H}\|_{1,\Omega} \lesssim (h + H^2)\|u\|_{W_2^{G,3}(\Omega)}, \tag{3.9}$$

$$\|u - u^h_{H,H,H}\|_{0,\Omega} \lesssim (h^2 + H^3)\|u\|_{W_2^{G,3}(\Omega)}. \tag{3.10}$$

Proof. The proof and the relative two-scale analysis are referred to the Appendix. □

It is concluded from Theorem 3.2 that the two-scale finite element combination approximation $u^h_{H,H,H}$ is a much more efficient approximate solution in terms of computational cost as compared to $u_{h,h,h}$. In fact, with the same approximate accuracy, the degrees of freedom for getting $u^h_{H,H,H}$ is only of $O(h^{-2})$ when $H = O(h^{1/2})$ is chosen while that for the standard finite element solution $u_{h,h,h}$ is of $O(h^{-3})$. In addition, it may be efficient that the two-scale finite element combination approximation $u^h_{H,H,H}$ can be carried out in parallel. As a result, both the computational time and the storage can be reduced. We therefore propose a refined two-scale finite element combination algorithm as follows.

Algorithm 3.2.

1. *Solve* (2.3) *on a coarse grid*: *Find* $u_{H,H,H} \in S_0^{H,H,H}(\Omega)$ *such that*

$$\mathcal{E}(u_{H,H,H}, v) = (f, v) \quad \textit{for all } v \in S_0^{H,H,H}(\Omega).$$

2. *Solve linear boundary value problems on partially fine grids in parallel*:

Find $e_{h,H,H} \in S_0^{h,H,H}(\Omega)$ *such that*

$$D(e_{h,H,H}, v) = (f, v) - \mathcal{E}(u_{H,H,H}, v) \quad \textit{for all } v \in S_0^{h,H,H}(\Omega);$$

Find $e_{H,h,H} \in S_0^{H,h,H}(\Omega)$ *such that*

$$D(e_{H,h,H}, v) = (f, v) - \mathcal{E}(u_{H,H,H}, v) \quad \textit{for all } v \in S_0^{H,h,H}(\Omega);$$

Find $e_{H,H,h} \in S_0^{H,H,h}(\Omega)$ *such that*

$$D(e_{H,H,h}, v) = (f, v) - \mathcal{E}(u_{H,H,H}, v) \quad \textit{for all } v \in S_0^{H,H,h}(\Omega).$$

3. *Set*

$$\widetilde{u}^h_{H,H,H} = u_{H,H,H} + e_{h,H,H} + e_{H,h,H} + e_{H,H,h} \quad \textit{in } \Omega.$$

4. *Find a further coarse grid correction* $\widehat{e}_{H,H,H} \in S_0^{H,H,H}(\Omega)$ *such that*

$$\mathcal{E}(\hat{e}_{H,H,H}, v) = (f, v) - \mathcal{E}(\widetilde{u}^h_{H,H,H}, v) \quad \textit{for all } v \in S_0^{H,H,H}(\Omega).$$

5. *Set* $\widehat{u}^h_{H,H,H} = \widetilde{u}^h_{H,H,H} + \widehat{e}_{H,H,H}$ *in* Ω.

Theorem 3.3. *Assume that* $\widetilde{u}^h_{H,H,H}$ *and* $\widehat{u}^h_{H,H,H}$ *are obtained by Algorithm* 3.2. *If* $u \in W_2^{G,3}(\Omega)$, *then*

$$\|u_{h,h,h} - \widetilde{u}^h_{H,H,H}\|_{1,\Omega} \lesssim H^2 \|u\|_{W_2^{G,3}(\Omega)}, \tag{3.11}$$

$$\|u_{h,h,h} - \widehat{u}^h_{H,H,H}\|_{0,\Omega} \lesssim H^3 \|u\|_{W_2^{G,3}(\Omega)}. \tag{3.12}$$

Consequently,

$$\|u - \widetilde{u}^h_{H,H,H}\|_{1,\Omega} \lesssim (h + H^2) \|u\|_{W_2^{G,3}(\Omega)}, \tag{3.13}$$

$$\|u - \widehat{u}^h_{H,H,H}\|_{0,\Omega} \lesssim (h^2 + H^3) \|u\|_{W_2^{G,3}(\Omega)}. \tag{3.14}$$

Proof. Set $u^{h,H,H} = u_{H,H,H} + e_{h,H,H}$, $u^{H,h,H} = u_{H,H,H} + e_{H,h,H}$ and $u^{H,H,h} = u_{H,H,H} + e_{H,H,h}$, then from the definition, we obtain $\widetilde{u}^h_{H,H,H} = u^{h,H,H} + u^{H,h,H} + u^{H,H,h} - 2u_{H,H,H}$. Hence,

$$\begin{aligned}
&\|u_{h,h,h} - \widetilde{u}^h_{H,H,H}\|_{1,\Omega} \\
&\quad \lesssim \|u^{h,H,H} + u^{H,h,H} + u^{H,H,h} - u_{h,H,H} - u_{H,h,H} - u_{H,H,h}\|_{1,\Omega} \\
&\qquad + \|u_{h,H,H} + u_{H,h,H} + u_{H,H,h} - 2u_{H,H,H} - u_{h,h,h}\|_{1,\Omega} \\
&\quad \lesssim \|u^{h,H,H} - u_{h,H,H}\|_{1,\Omega} + \|u^{H,h,H} - u_{H,h,H}\|_{1,\Omega} \\
&\qquad + \|u^{H,H,h} - u_{H,H,h}\|_{1,\Omega} + \|u_{h,H,H} + u_{H,h,H} + u_{H,H,h} \\
&\qquad - 2u_{H,H,H} - u_{h,h,h}\|_{1,\Omega}.
\end{aligned}$$

Note that Theorem 3.1 implies

$$\begin{aligned}\|u^{h,H,H} - u_{h,H,H}\|_{1,\Omega} + \|u^{H,h,H} - u_{H,h,H}\|_{1,\Omega} \\ + \|u^{H,H,h} - u_{H,H,h}\|_{1,\Omega} \\ \lesssim H^2\|u\|_{2,\Omega}.\end{aligned} \tag{3.15}$$

Therefore, combining (3.15) and Theorem 3.2, we get (3.11) and then (3.13). The following holds

$$\begin{aligned}\|u_{h,h,h} - \widehat{u}^h_{H,H,H}\|_{0,\Omega} &= \|(I - P_{H,H,H})(u_{h,h,h} - \widetilde{u}^h_{H,H,H})\|_{0,\Omega} \\ &\lesssim H\|u_{h,h,h} - \widetilde{u}^h_{H,H,H}\|_{1,\Omega}.\end{aligned}$$

This completes the proof. □

Remark 3.3. We may also develop some local and parallel algorithms for the combination based two-scale finite element method (cf., [**29**]).

Remark 3.4. The combination based two-scale discretization approach can be generalized to any dimension. For $\Omega = [0,1]^d$ $(d \geq 2)$, recall that the standard Galerkin projection $P_{\mathbf{h}} : H_0^1(\Omega) \mapsto S_0^{\mathbf{h}}(\Omega)$ is defined by

$$\mathcal{E}(u - P_{\mathbf{h}}u, v) = 0 \quad \text{for all } v \in S_0^{\mathbf{h}}(\Omega) \tag{3.16}$$

for $\mathbf{h} = (h_1, h_2, \ldots, h_d)$. Then we can construct the two-scale finite element Galerkin projection as follows:

$$B^h_{H\mathbf{e}}P_{h\mathbf{e}}u = \sum_{i=1}^{d} P_{H\widehat{\mathbf{e}}_i + h\mathbf{e}_i}u - (d-1)P_{H\mathbf{e}}u,$$

where $\mathbf{e} = (1, \ldots, 1) \in \mathbf{R}^d$, $\widehat{\mathbf{e}}_i = \mathbf{e} - \mathbf{e}_i$, $\mathbf{e}_i = (0, \ldots, 0, 1, 0, \ldots, 0) \in \mathbf{R}^d$ whose i-th component is one and zero otherwise, and $\mathbf{h}\alpha = (h_1\alpha_1, \ldots, h_d\alpha_d)$ for $\alpha_i \in \{0, 1\}$, $i \in \{1, 2, \ldots, d\}$. For instance, $B^h_{H,H,H}P_{h,h,h}u = P_{h,H,H}u + P_{H,h,H}u + P_{H,H,h}u - 2P_{H,H,H}u$. Following [**20**], we can expect similar results for $d-$dimensions. For instance, if $u \in H_0^1(\Omega) \cap W_2^{G,3}(\Omega)$, then

$$\begin{aligned}\|B^h_{H\mathbf{e}}P_{h\mathbf{e}}u - P_{h\mathbf{e}}u\|_{0,\Omega} + H\|B^h_{H\mathbf{e}}P_{h\mathbf{e}}u - P_{h\mathbf{e}}u\|_{1,\Omega} \\ \lesssim H^3\|u\|_{W_2^{G,3}(\Omega)}.\end{aligned} \tag{3.17}$$

3.2. Wavelet-Lagrangian two-scale discretization. In this subsection, we will briefly describe how the advantages of wavelet-based methods can be combined with the two-scale algorithms presented before. As already indicated in the introduction, the basic idea behind this approach is the following: At first, a wavelet discretization yields an almost sparse representation of the non-local form $J(\cdot,\cdot)$ defined by (2.6) (see, e.g., [**13, 35, 39**]). Secondly, as illustrated in the above sections, the local form $D(\cdot,\cdot)$ can be discretized very efficiently with significantly less computational overhead using plain Lagrangian basis functions or, alternatively, single scale bases made up by splines. In order to minimize the computational overhead these bases should be chosen as simple as possible.

In order to exploit both the advantages of the wavelet basis and the classical Lagrangian basis, Algorithms 3.1 and 3.2 can be realized by

Algorithm 3.3.

1. *For the coarse grid discretization of the form*

$$\text{Find } u_H \in S_0^H(\Omega) \text{ such that } \mathcal{E}(u_H, v) = (f, v) \quad \text{for all } v \in S_0^H(\Omega),$$

employ the sparse tensor product wavelet methods of [**19**] *with additional wavelet compression as in* [**31, 35**] *to efficiently obtain the wavelet representation*

$$u_H = \sum_{j'=0}^{J} \sum_{k' \in \nabla_{j'}} d^H_{j',k'} \psi_{j',k'},$$

where $H = 2^{-J}$.

2. *Employ the multiscale transformation* $\mathbf{T}_j \mathbf{d}^H$ *to obtain the corresponding single-scale representation of* u_H *in terms of Lagrangian basis functions with coefficient vector* $\mathbf{c}^H$ *as in* (2.21).

3. *Proceed with the two-scale discretization algorithm from Step* 2 *in Algorithms* 3.1 *or* 3.2. *In particular, use existing methodology of, e.g.,* [**20, 28, 29**] *to efficiently discretize the local form* $D(\cdot,\cdot)$ *on the fine grid.*

4. *Make further corrections on the coarse grid by using the inverse of multiscale transform and sparse tensor product wavelets methods.*

The main reason for combining wavelet methods with classical finite element methods in the above algorithms is the non-locality of the form $\mathcal{E}(\cdot,\cdot)$ due to existence of the jump part. Even on the coarse grid, standard finite element schemes are of complexity $\mathcal{O}(H^{-2d})$ and therefore hard to apply even in moderate dimensions. It is known however that sparse tensor product wavelets yield a quasi-sparse representation even of non-local bilinear forms resulting in asymptotically optimal complexity $\mathcal{O}(H^{-1}|\log H|^{2(d-1)})$ (see, e.g., [**19, 35**]). For the fine-grid discretization of $D(\cdot,\cdot)$ one may still employ the same wavelet methods, but, since the form is local, for moderate dimensions one obtains an efficient discretization with well structured sparse stiff matrix and significantly less computational overhead by using Algorithms 3.1 and 3.2 with Lagrangian finite element functions (or, alternatively, single scale bases made up by splines).

3.4. Parabolic problems. In this subsection, we briefly illustrate how to discretize the time-dependent problems derived from Lévy copula process in finance. We consider the following backward Kolmogorov equation:

$$\begin{cases} \frac{\partial u(t,x)}{\partial t} + \mathcal{A}u(t,x) = f(t,x) & \text{in } (0,T)\times\Omega, \\ u(t,x) = 0 & \text{on } (0,T)\times\partial\Omega, \\ u(0,x) = u_0(x) & \text{in } \Omega, \end{cases} \tag{3.18}$$

where $\mathcal{A}$ is the (integro-differential) infinitesimal generator of the Lévy process.

The variational form of the parabolic problem (3.18) reads: Find $u \in L^2((0,T);H^1(\Omega)) \cap H^1((0,T);H^{-1}(\Omega))$ such that

$$\begin{cases} \left\langle \frac{\partial u}{\partial t}, v \right\rangle_{(H^{-1}(\Omega),H^1(\Omega))} + \mathcal{E}(u,v) = (f,v) & \text{in } (0,T)\times\Omega, \\ & \text{for all } v \in H_0^1(\Omega), \\ u\,|_{t=0} = u_0, \end{cases} \tag{3.19}$$

where $\mathcal{E}(u,v)$ is given by (2.4).

Assume that a finite-dimensional space $V^h \subset H^1(\Omega)$ corresponding to a given meshwidth $h > 0$ has been fixed, we can then use the θ-scheme for time discretization. Let $0 \le \theta \le 1$. For $T < \infty$ and $M \in \mathbf{N}$

define the time step $k = T/M$, and $t^m = mk$, $m = 0, 1, \ldots, M$. The fully discrete θ-scheme reads:

Algorithm 3.4.

1. *Find $u_h^0 \in V^h$ satisfying $u_h^0 = u_{0,h}$. The approximation of the initial data could be chosen as a finite element projection $u_{0,h} = P_h u_0$ or as an interpolant of u_0.*

2. *For $m = 0, 1, \ldots, M-1$, find $u_h^{m+1} \in V^h$ such that*

$$\left(\frac{u_h^{m+1} - u_h^m}{k}, v_h\right) + \mathcal{E}(u_h^{m+\theta}, v_h) = (f, v_h) \quad \text{for all } v_h \in V^h, \tag{3.20}$$

where $u_h^{m+\theta} := \theta u_h^{m+1} + (1-\theta) u_h^m$.

For $\theta = 1/2$, the scheme in (3.20) coincides with the Crank-Nicholson scheme, whereas for $\theta = 0$ one obtains the explicit and for $\theta = 1$ the implicit Euler scheme. For stability and convergence considerations we refer to [**31, 39**]. In practice, more sophisticated tools, e.g., *hp*-DG time-stepping (see [**24**]), can be applied to obtain exponential convergence in time.

Note that for each time step m of the fully discrete θ-scheme, (3.20) is equivalent to solving an elliptic problem: Find $u^{m+1} \in H_0^1(\Omega)$ such that

$$\widehat{\mathcal{E}}(u^{m+1}, v) = (\widehat{f}(u^m), v) \quad \text{for all } v \in H_0^1(\Omega), \tag{3.21}$$

where the bilinear form $\widehat{\mathcal{E}}(\cdot,\cdot)$ and $(\widehat{f}, v)$ are given by:

$$\widehat{\mathcal{E}}(u^{m+1}, v) = \theta \mathcal{E}(u^{m+1}, v) + \frac{1}{k}(u^{m+1}, v),$$
$$(\widehat{f}(u^m), v) = \frac{1}{k}(u^m, v) - (1-\theta)\mathcal{E}(u^m, v) + (f, v).$$

Therefore, we have to solve an elliptic problem (3.21) at each time step, and the algorithms presented in subsections 3.1–3.3 can be applied to reduce the computational cost.

4. Numerical experiments. In this section, we will present some numerical experiments which support the theories in the previous

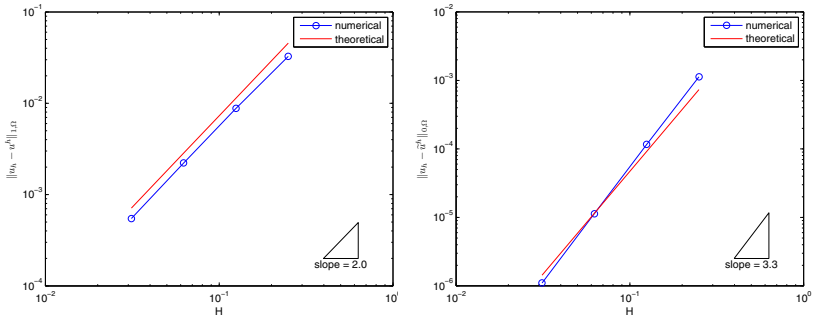

FIGURE 2. Basic two-scale scheme for one-dimensional elliptic problem.

sections. In order to compute the error, we consider the function, $w : \mathbf{R} \to \mathbf{R}$,

$$w(x) = \begin{cases} x^5 - x^4 - x^3 + x^2 & \text{if } x \in (0,1), \\ 0 & \text{else.} \end{cases}$$

Clearly $w \in H^2(0,1)$ in the sense of (2.1). In the numerical experiments, we use the piecewise linear Lagrangian finite element described in Section 2.2. All computations are performed in double precision arithmetic on a PC with 2GB in Matlab 8.0.

Example 1. Consider a one-dimensional elliptic problem

$$\mathcal{E}(u,v) = (f,v) \quad \text{for all } v \in H_0^1(\Omega),$$

where $\Omega = (0,1)$, $D(u,v) = \int_0^1 u'(x)v'(x)\,dx$,

$$J(u,v) = -\int_0^1 \int_{\mathbf{R}} \left(u(x+z) - u(x)\right) v(x)\,dx\; k(z)\,dz.$$

TABLE 1. Basic two-scale scheme for one-dimensional elliptic problem.

$L(h = 2^{-2L}, H = 2^{-L})$	$\|u - u_h\|_{1,\Omega}$	$\|u - u^h\|_{1,\Omega}$	$\|u - u_h\|_{0,\Omega}$	$\|u - \tilde{u}^h\|_{0,\Omega}$
2	0.03656280	0.04728101	0.00129277	0.00053462
3	0.00906203	0.01247740	0.00008560	0.00005595
4	0.00225810	0.00315163	0.00000544	0.00000707
5	0.00056399	0.00078517	0.00000032	0.00000084
convergence rate	$\mathcal{O}(h)$	$\mathcal{O}(h)$ or $\mathcal{O}(H^2)$	$\mathcal{O}(h^2)$	$\mathcal{O}(h^{3/2})$ or $\mathcal{O}(H^3)$

and $k(z) = |z|^{-1-\alpha}$. We take $\alpha = 0.8$ and choose f such that $u(x) = w(x)$ is the exact solution. To illustrate the convergence rate in Theorem 3.1, we compute $\|u_h - u^h\|_{1,\Omega}$ and $\|u_h - \widetilde{u}^h\|_{0,\Omega}$ at each level, and plot them in Figure 2. We see from the pictures that the convergence rates are exactly the same as that of our stated theory. Table 1 compares the errors between two-scale and one-scale schemes, which suggest that the two-scale discretization can achieve the same accuracy with lower computational cost.

Example 2. Consider a two-dimensional problem, and choose f such that $u(x, y) = w(x)w(y)$ is the exact solution of

$$\mathcal{E}(u, v) = (f, v) \quad \text{for all } v \in H_0^1(\Omega),$$

where $\Omega = (0, 1)^2$,

$$D(u, v) = \int_0^1 \int_0^1 \left(\frac{\partial u}{\partial x} \frac{\partial v}{\partial x} + \frac{\partial u}{\partial y} \frac{\partial v}{\partial y} \right) dx\, dy,$$

$$\begin{aligned} J(u, v) = &- \int_\Omega \int_{\mathbf{R}} (u(x + z, y) - u(x, y))\, v(x, y)\, dx\, dy\; k_1(z)\, dz \\ &- \int_\Omega \int_{\mathbf{R}} (u(x, y + z) - u(x, y))\, v(x, y)\, dx\, dy\; k_2(z)\, dz, \end{aligned}$$

and $k_i(z) = |z|^{-1-\alpha_i}$, $i = 1, 2$. Letting $\alpha_1 = 1.1$ and $\alpha_2 = 1.2$, we display the convergence rate of $\|u_h - u^h\|_{1,\Omega}$ and $\|u_h - \widetilde{u}^h\|_{0,\Omega}$ in Figure 3 and compare the errors between the two-scale and one-scale schemes in Table 2. Note that in this example $\alpha_i > 1$ $(i = 1, 2)$, which does not

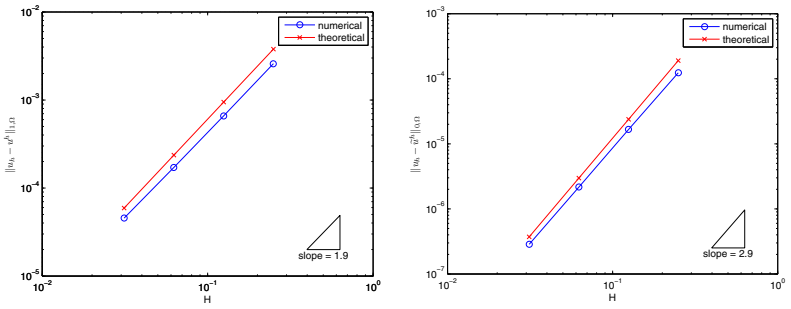

FIGURE 3. Basic two-scale scheme for two-dimensional elliptic problem.

TABLE 2. Basic two-scale scheme for two-dimensional elliptic problem.

$L(h=2^{-L-1}, H=2^{-L})$	$\|u-u_h\|_{1,\Omega}$	$\|u-u^h\|_{1,\Omega}$	$\|u-u_h\|_{0,\Omega}$	$\|u-\tilde{u}^h\|_{0,\Omega}$
2	0.004220	0.004723	0.000189	0.000185
3	0.002130	0.002204	0.000047	0.000043
4	0.001067	0.001078	0.000012	0.000011
5	0.000534	0.000535	0.000003	0.000003
convergence rate	$\mathcal{O}(h)$	$\mathcal{O}(h)$	$\mathcal{O}(h^2)$	$\mathcal{O}(h^2)$

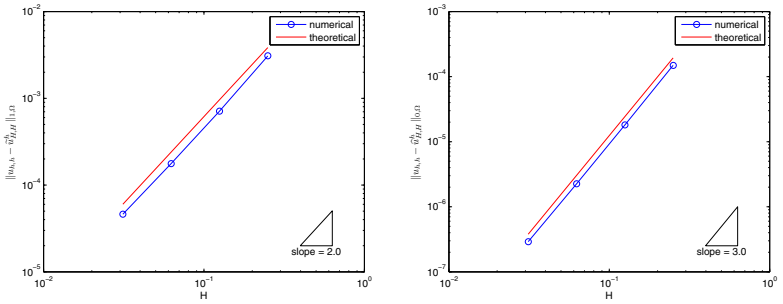

FIGURE 4. Combination based two-scale scheme for two-dimensional elliptic problem.

TABLE 3. Combination based two-scale scheme for two-dimensional elliptic problem.

$L(h=2^{-L-1}, H=2^{-L})$	$\|u-u_{h,h}\|_{1,\Omega}$	$\|u-\tilde{u}^h_{H,H}\|_{1,\Omega}$	$\|u-u_{h,h}\|_{0,\Omega}$	$\|u-\tilde{u}^h_{H,H}\|_{0,\Omega}$
2	0.004220	0.004991	0.000189	0.000202
3	0.002130	0.002220	0.000047	0.000043
4	0.001067	0.001079	0.000012	0.000011
5	0.000534	0.000536	0.000003	0.000003
convergence rate	$\mathcal{O}(h)$	$\mathcal{O}(h)$	$\mathcal{O}(h^2)$	$\mathcal{O}(h^2)$

satisfy Assumption 2.1, but we still get reasonable results which illustrate the efficiency of our two-scale discretization scheme.

The combination based two-scale methods are also implemented in this two-dimensional example. The convergence rate of $\|u_{h,h} -$

$\|\widetilde{u}^h_{H,H}\|_{1,\Omega}$ and $\|u_{h,h} - \widehat{u}^h_{H,H}\|_{0,\Omega}$ are shown in Figure 4, which is consistent with Theorem 3.3. We also compare the errors of the combination based two-scale scheme and the one-scale scheme in Table 3.

Example 3. A three-dimensional problem is calculated in this example. We choose f such that $u(x_1, x_2, x_3) = w(x_1)w(x_2)w(x_3)$ is the exact solution of

$$\mathcal{E}(u, v) = (f, v) \quad \text{for all } v \in H_0^1(\Omega),$$

where $\Omega = (0,1)^3$, $D(u,v) = \sum_{i=1}^{3} \int_\Omega \frac{\partial u}{\partial x_i} \frac{\partial v}{\partial x_i}$,

$$\begin{aligned} J(u,v) = &- \int_\Omega \int_{\mathbf{R}} (u(x_1 + z, x_2, x_3) \\ &- u(x_1, x_2, x_3))v(x_1, x_2, x_3)\, dx_1\, dx_2\, dx_3\, k_1(z)\, dz \\ &- \int_\Omega \int_{\mathbf{R}} (u(x_1, x_2 + z, x_3) \\ &- u(x_1, x_2, x_3))v(x_1, x_2, x_3)\, dx_1\, dx_2\, dx_3\, k_2(z)\, dz \\ &- \int_\Omega \int_{\mathbf{R}} (u(x_1, x_2, x_3 + z) \\ &- u(x_1, x_2, x_3))v(x_1, x_2, x_3)\, dx_1\, dx_2\, dx_3\, k_3(z)\, dz, \end{aligned}$$

and $k_i(z) = |z|^{-1-\alpha_i}$, $i = 1, 2, 3$. We take $\alpha_1 = 0.5$, $\alpha_2 = 0.8$, $\alpha_3 = 1.2$ and briefly examine the basic two-scale and the combination based two-scale scheme respectively by displaying the convergence rate of $\|u_h - u^h\|_{1,\Omega}$ and $\|u_{h,h,h} - \widetilde{u}^h_{H,H,H}\|_{1,\Omega}$ in Figure 5, which is consistent with Theorems 3.1 and 3.3.

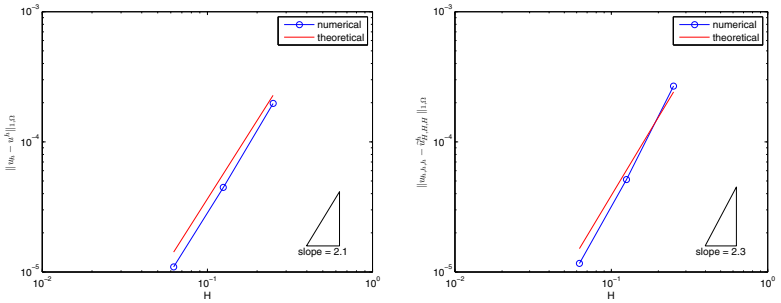

FIGURE 5. Two-scale scheme for three-dimensional elliptic problem.

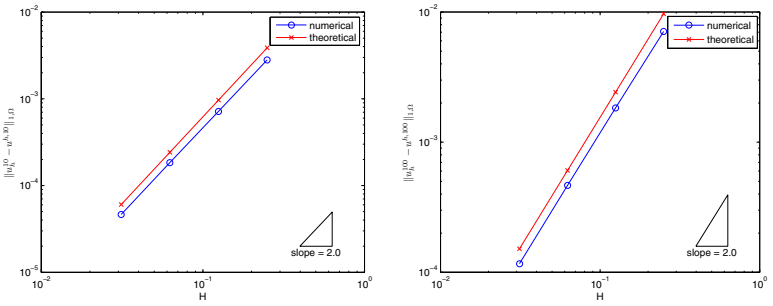

FIGURE 6. Two-scale discretization scheme for parabolic problem.

Example 4. Finally, consider a two-dimensional parabolic problem:

$$\begin{cases} \left(\frac{\partial u}{\partial t}, v\right) + \mathcal{E}(u,v) = (f,v) & \text{in } (0,T)\times\Omega, \text{ for all } v \in H_0^1(\Omega) \\ u|_{t=0} = u_0 & \text{in } \Omega, \end{cases}$$

where $\Omega = (0,1)^2$,

$$D(u,v) = \int_\Omega \left(\frac{\partial u}{\partial x}\frac{\partial v}{\partial x} + \frac{\partial u}{\partial y}\frac{\partial v}{\partial y} \right) dx\, dy,$$

$$\begin{aligned} J(u,v) = &- \int_\Omega \int_{\mathbf{R}} \left(u(x+z,y) - u(x,y)\right) v(x,y)\, dx\, dy\; k_1(z)\, dz \\ &- \int_\Omega \int_{\mathbf{R}} \left(u(x,y+z) - u(x,y)\right) v(x,y)\, dx\, dy\; k_2(z)\, dz, \end{aligned}$$

and $k_i(z) = |z|^{-1-\alpha_i}$, $i = 1,2$. We take $\alpha_1 = 0.8$, $\alpha_2 = 0.9$ and choose $f(t,x,y)$ such that $u(t,x,y) = e^t w(x) w(y)$ is the exact solution of the problem. Letting $k = 0.01$ and $\theta = 0.5$ in (3.20), we display the convergence rate of $\|u_h^m - u^{h,m}\|_{1,\Omega}$ at time $T = mk$ $(m = 10, 100)$ in Figure 6, which supports that our two-scale algorithm is also efficient for time-dependent problems.

APPENDIX

Let $I_{h_{x_1},h_{x_2},h_{x_3}}$ be the usual trilinear interpolation operator on the tensor product mesh $T^{h_{x_1},h_{x_2},h_{x_3}}(\Omega)$. One sees that $I_{h_{x_1},0,0}$ is the

interpolation operator which interpolates only in the x_1-direction on lines of mesh size h_{x_1}, etc. Obviously,

$$I_{h_{x_1},h_{x_2},h_{x_3}} = I_{h_{x_1},0,0} \cdot I_{0,h_{x_2},0} \cdot I_{0,0,h_{x_3}}.$$

It is shown in the following lemma that a one-scale interpolation on a fine grid can be obtained by a combination of two-scale interpolations asymptotically. Let $H \gg h$, and define the two-scale interpolation by

$$I^h_{H,H,H}u = I_{h,H,H}u + I_{H,h,H}u + I_{H,H,h}u - 2I_{H,H,H}u.$$

From the identity

$$\begin{aligned} I = {} & I_{h,h,h} + (I - I_{h,0,0}) + (I - I_{0,h,0}) + (I - I_{0,0,h}) \\ & - (I - I_{h,0,0})(I - I_{0,h,0}) - (I - I_{h,0,0})(I - I_{0,0,h}) \\ & - (I - I_{0,h,0})(I - I_{0,0,h}) + (I - I_{h,0,0})(I - I_{0,h,0})(I - I_{0,0,h}), \end{aligned}$$

we obtain the following two results (see [**28**] for details).

Lemma A.1 [**28**]. *If $u \in W_2^{G,3}(\Omega)$, then*

(A.1)
$$H\|I^h_{H,H,H}u - I_{h,h,h}u\|_{1,\Omega} + \|I^h_{H,H,H}u - I_{h,h,h}u\|_{0,\Omega} \lesssim H^3\|u\|_{W_2^{G,3}(\Omega)}.$$

Lemma A.2 [**28**]. *If $u \in H_0^1(\Omega) \cap W_2^{G,3}(\Omega)$, then*

(A.2)
$$D((I - I_{h_{x_1},h_{x_2},h_{x_3}})u, v) \lesssim (\max\{h_{x_1}, h_{x_2}, h_{x_3}\})^2\|u\|_{W_2^{G,3}(\Omega)}\|v\|_{1,\Omega}$$
$$\text{for all } v \in S_0^{h_{x_1},h_{x_2},h_{x_3}}(\Omega).$$

Proof of Theorem 3.2. Recall that the two-scale finite element combination approximation (3.6):

$$u^h_{H,H,H} = u_{h,H,H} + u_{H,h,H} + u_{H,H,h} - 2u_{H,H,H}.$$

By the triangle inequality, we have

$$
\begin{aligned}
(A.3)\quad & \|u_{h,h,h} - u^h_{H,H,H}\|_{1,\Omega} \\
& \lesssim \|u_{h,H,H} - I_{h,H,H}u\|_{1,\Omega} + \|u_{H,h,H} - I_{H,h,H}u\|_{1,\Omega} \\
& \quad + \|u_{H,H,h} - I_{H,H,h}u\|_{1,\Omega} + 2\|u_{H,H,H} - I_{H,H,H}u\|_{1,\Omega} \\
& \quad + \|u_{h,h,h} - I_{h,h,h}u\|_{1,\Omega} \\
& \quad + \|I_{h,H,H}u + I_{H,h,H}u + I_{H,H,h}u - 2I_{H,H,H}u - I_{h,h,h}u\|_{1,\Omega}.
\end{aligned}
$$

Next, we want to estimate $\|u_{h,H,H} - I_{h,H,H}u\|_{1,\Omega}$. For all $v \in S_0^{h,H,H}(\Omega)$, the following holds

$$
\begin{aligned}
\mathcal{E}(u_{h,H,H} - I_{h,H,H}u, v) &= \mathcal{E}(u - I_{h,H,H}u, v) \\
&= D(u - I_{h,H,H}u, v) + J(u - I_{h,H,H}u, v).
\end{aligned}
$$

Using Lemma 2.2 and Lemma A.2, we then obtain

$$
\begin{aligned}
&\mathcal{E}(u_{h,H,H} - I_{h,H,H}u, v) \\
&\qquad \lesssim H^2\|u\|_{W_2^{G,3}(\Omega)}\|v\|_{1,\Omega} + \|u - I_{h,H,H}u\|_{0,\Omega}\|v\|_{1,\Omega} \\
&\qquad \lesssim H^2\|u\|_{W_2^{G,3}(\Omega)}\|v\|_{1,\Omega}.
\end{aligned}
$$

Choosing $v := u_{h,H,H} - I_{h,H,H}u$ and applying (2.10), we get

$$
(A.4)\qquad \|u_{h,H,H} - I_{h,H,H}u\|_{1,\Omega} \lesssim H^2\|u\|_{W_2^{G,3}(\Omega)},
$$

which together with Lemma A.1 and similar estimations of the other terms in (A.3) yields (3.7).

For the L^2-norm error estimate, we use a duality argument. Let $w \in H_0^1(\Omega)$ such that

$$
\mathcal{E}(w, \phi) = (u_{h,h,h} - u^h_{H,H,H}, \phi) \quad \text{for all } \phi \in H_0^1(\Omega).
$$

Let $\phi := u_{h,h,h} - u^h_{H,H,H} \in H_0^1(\Omega)$. Then we have

$$
\begin{aligned}
&(u_{h,h,h} - u^h_{H,H,H}, u_{h,h,h} - u^h_{H,H,H}) \\
&\qquad = \mathcal{E}(w, u_{h,h,h} - u^h_{H,H,H}) \\
&\qquad = \mathcal{E}(u_{h,h,h} - u^h_{H,H,H}, w - I_{H,H,H}w) \\
&\qquad \lesssim \|u_{h,h,h} - u^h_{H,H,H}\|_{1,\Omega}\|w - I_{H,H,H}w\|_{1,\Omega}.
\end{aligned}
$$

Since $\|w - I_{H,H,H}w\|_{1,\Omega} \lesssim H|w|_{2,\Omega} \lesssim H\|u_{h,h,h} - u^h_{H,H,H}\|_{0,\Omega}$, we arrive at

$$\|u_{h,h,h} - u^h_{H,H,H}\|_{0,\Omega} \lesssim H\|u_{h,h,h} - u^h_{H,H,H}\|_{1,\Omega} \lesssim H^3\|u\|_{W_2^{G,3}(\Omega)}.$$

By the triangle inequality, we complete the proof. □

Acknowledgments. The authors would like to thank Professor C. Schwab of ETH Zürich for valuable comments and discussions.

REFERENCES

1. O.E. Barndorff-Nielsen, *Normal inverse Gaussian distributions and stochastic volatility modelling*, Scand. J. Statist. **24** (1997), 1–13.

2. J.H. Bramble, *Multigrid methods*, Pitman Res. Notes Math. **294**, London Co, published in the USA with Wiley, New York, 1993.

3. M. Briani, R. Natalini and G. Russo, *Implicit-explicit numerical schemes for jump–diffusion processes*, Calcolo **44** (2007), 33–57.

4. H.J. Bungartz and M. Griebel, *Sparse grids*, Acta Numer. **13** (2004), 1–123.

5. H.J. Bungartz, M. Griebel and U. Rüde, *Extrapolation, combination, and sparse grid techniques for elliptic boundary value problems*, Comput. Methods Appl. Mech. Engrg. **116** (1994), 243–252.

6. J.M. Carnicer, W. Dahmen and J.M. Peña, *Local decomposition of refinable spaces and wavelets*, Appl. Comput. Harmon. Anal. **3** (1996), 127–153.

7. P. Carr, H. Geman, D.B. Madan and M. Yor, *The fine structure of assets returns: An empirical investigation*, J. Business **75** (2002), 305–332.

8. P.G. Ciarlet, *Basic error estimates for elliptic problems*, in *Handbook of numerical analysis* Vol. II, North-Holland, Amsterdam, 1991.

9. A. Cohen, *Numerical analysis of wavelet methods*, Stud. Math. Appl. **32**, North-Holland Publishing Co., Amsterdam, 2003.

10. R. Cont and E. Voltchkova, *A finite difference scheme for option pricing in jump diffusion and exponential Lévy models*, SIAM J. Numer. Anal. **43** (2005), 1596–1626.

11. W. Dahmen, *Stability of multiscale transformations*, J. Fourier Anal. Appl. **2** (1996), 341–361.

12. ———, *Multiscale and wavelet methods for operator equations*, in *Multiscale problems and methods in numerical simulations*, Lecture Notes in Math. **1825**, Springer, Berlin, 2003.

13. W. Dahmen, H. Harbrecht and R. Schneider, *Compression techniques for boundary integral equations–Asymptotically optimal complexity estimates*, SIAM J. Numer. Anal. **43** (2006), 2251–2271.

14. W. Dahmen, A. Kunoth and K. Urban, *Biorthogonal spline wavelets on the interval-stability and moment conditions*, Appl. Comput. Harm. Anal. **6** (1999), 259–302.

15. W. Dahmen, S. Prößdorf and R. Schneider, *Wavelet approximation methods for periodic pseudodifferential equations*, Part II–*Fast solution and matrix compression*, Adv. Comput. Math. **1** (1193), 259–335.

16. F. Delbaen, P. Grandits, T. Rheinländer, D. Samperi, M. Schweizer and C. Stricker, *Exponential hedging and entropic penalties*, Math. Finance **12** (2002), 99–123.

17. F. Delbaen and W. Schachermayer, *A general version of the fundamental theorem of asset pricing*, Math. Ann. **300** (1994), 463–520.

18. E. Eberlein and J. Jacod, *On the range of options prices*, Finance Stoch. **1** (1997), 131–140.

19. W. Farkas, N. Reich and C. Schwab, *Anisotropic stable Lévy copula processes–Analytical and numerical aspects*, Math. Model. Methods Appl. Sci. **17** (2007), 1405–1443.

20. X. Gao, F. Liu and A. Zhou, *Three-scale finite element discretization schemes for eigenvalue problems*, BIT Numer. Math. **48** (2008), 533–562.

21. V. Girault and J.L. Lions, *Two-grid finite element schemes for the transient Navier-Stokes problem*, M2AN Math. Model. Numer. Anal., **35** (2001), 945–980.

22. M. Griebel, P. Oswald and T. Schiekofer, *Sparse grids for boundary integral equations*, Numer. Math. **83** (1999), 279–312.

23. W. Hackbusch, *Multigrid methods and applications*, Springer Ser. Comp. Math. **4**, Springer-Verlag, Berlin, 1985.

24. N. Hilber, A.M. Matache and C. Schwab, *Sparse wavelet methods for option pricing under stochastic volatility*, J. Comput. Finance **8** (2005), 1–42.

25. J. Kallsen and P. Tankov, *Characterization of dependence of multidimensional Lévy processes using Lévy copulas*, J. Multivariate Anal. **97** (2006), 1551–1572.

26. G. Kou, *A jump diffusion model for option pricing*, Mange. Sci. **48** (2002), 1086–1101.

27. W. Layton and L. Tobiska, *A two-level method with backtracking for the Navier-Stokes equations*, SIAM J. Numer. Anal. **35** (1998), 2035–2054.

28. F. Liu and A. Zhou, *Two-scale finite element discretizations for partial differential equations*, J. Comput. Math. **24** (2006), 373–392.

29. ———, *Localizations and parallelizations for two-scale finite element discretizations*, Comm. Pure Appl. Anal. **6** (2007), 757–773.

30. ———, *Two-scale Boolean Galerkin discretizations for Fredholm integral equations of the second kind*, SIAM J. Numer. Anal. **45** (2007), 296–312.

31. A.M. Matache, T. von Petersdorff and C. Schwab, *Fast deterministic pricing of options on Lévy driven assets*, M2AN Math. Model. Numer. Anal. **38** (2004), 37–71.

32. M. Mu and J. Xu, *A two-grid method of a mixed Stokes-Darcy model for coupling fluid flow with porous media flow*, SIAM J. Numer. Anal. **45** (2007), 1801–1813.

33. H. Nguyen and R. Stevenson, *Finite-element wavelets on manifolds*, IMA J. Numer. Math. **23** (2003), 149–173.

34. C. Pflaum and A. Zhou, *Error analysis of the combination technique*, Numer. Math. **84** (1999), 327–350.

35. N. Reich, *Wavelet compression of anisotropic integrodifferential operators on sparse tensor product spaces*, Ph.D. thesis 17661, ETH Zürich, 2008.

36. N. Reich, C. Schwab and C. Winter, *On Kolmogorov equations for anisotropic multivariate Lévy processes*, Finance Stoch., 2010, to appear.

37. K. Sato, *Lévy processes and infinitely divisible distributions*, Cambridge Stud. Adv. Math. **68**, Cambridge University Press, Cambridge, 1999.

38. W. Schoutens, *Lévy processes in finance*, John Wiley & Sons, Chichester, 2003.

39. T. von Petersdorff and C. Schwab, *Wavelet discretizations of parabolic integro-differential equations*, SIAM J. Numer. Anal. **41** (2003), 159–180.

40. ———, *Numerical solution of parabolic equations in high dimensions*, M2AN Math. Model. Numer. Anal. **38** (2004), 93–127.

41. J. Xu, *Iterative methods by space decomposition and subspace correction*, SIAM Rev. **34** (1992), 581–613.

42. ———, *Two-grid discretization techniques for linear and nonlinear* PDEs, SIAM J. Numer. Anal. **33** (1996), 1759–1777.

43. J. Xu and A. Zhou, *Local and parallel finite element algorithms based on two-grid discretizations*, Math. Comput. **69** (2000), 881–909.

44. ———, *Local and parallel finite element algorithms based on two-grid discretizations for nonlinear problems*, Adv. Comput. Math. **14** (2001), 293–327.

45. H. Yserentant, *On the multi-level splitting of finite element spaces*, Numer. Math. **49** (1986), 379–412.

46. C. Zenger, *Sparse grids*, in *Parallel algorithms for partial differential equations*, Notes Numer. Fluid Mech. **31**, Vieweg, Braunschweig, 1991.

LSEC, Institute of Computational Mathematics and Scientific/Engineering Computing, Academy of Mathematics and Systems Science, Chinese Academy of Sciences, Beijing 100190, China
Email address: hjchen@lsec.cc.ac.cn

School of Applied Mathematics, Central University of Finance and Economics, Beijing 100081, China
Email address: fliu@lsec.cc.ac.cn

Seminar for Applied Mathematics, ETH Zürich, 8092 Zürich, Switzerland
Email address: reich@math.ethz.ch

Seminar for Applied Mathematics, ETH Zürich, 8092 Zürich, Switzerland
Email address: chwinter@math.ethz.ch

LSEC, Institute of Computational Mathematics and Scientific/Engineering Computing, Academy of Mathematics and Systems Science, Chinese Academy of Sciences, Beijing 100190, China
Email address: azhou@lsec.cc.ac.cn